Trojan particles: Large porous carriers of nanoparticles for drug delivery

N. Tsapis*, D. Bennett†, B. Jackson†, D. A. Weitz*, and D. A. Edwards*‡

*Department of Physics, and Division of Engineering and Applied Sciences, Harvard University, 9 Oxford Street, Cambridge, MA 02138; and †Alkermes, Inc., 88 Sydney Street, Cambridge, MA 02139

Edited by Andreas Acrivos, City College of the City University of New York, New York, NY, and approved July 16, 2002 (received for review April 18, 2002)

We have combined the drug release and delivery potential of nanoparticle (NP) systems with the ease of flow, processing, and aerosolization potential of large porous particle (LPP) systems by spray drying solutions of polymeric and nonpolymeric NPs into extremely thin-walled macroscale structures. These hybrid LPPs exhibit much better flow and aerosolization properties than the NPs; yet, unlike the LPPs, which dissolve in physiological conditions to produce molecular constituents, the hybrid LPPs dissolve to produce NPs, with the drug release and delivery advantages associated with NP delivery systems. Formation of the large porous NP (LPNP) aggregates occurs via a spray-drying process that ensures the drying time of the sprayed droplet is sufficiently shorter than the characteristic time for redistribution of NPs by diffusion within the drying droplet, implying a local Peclet number much greater than unity. Additional control over LPNPs physical characteristics is achieved by adding other components to the spray-dried solutions, including sugars, lipids, polymers, and proteins. The ability to produce LPNPs appears to be largely independent of molecular component type as well as the size or chemical nature of the NPs.

Large porous particles (LPPs), characterized by geometric sizes larger than 5 μm and mass densities around 0.1 g/cm^3 or less, have achieved recent popularity as carriers of drugs to the lungs for local and systemic applications (1, 2). A principal advantage of LPPs relative to conventional inhaled therapeutic aerosol particles is their aerosolization efficiency (3, 4); in addition, LPPs possess the potential for avoidance of alveolar macrophage clearance (5–7), enabling sustained drug release in the lungs (8).

Particles with geometric diameters less than a few hundred nanometers (9) represent an even more tenacious resident of the lungs. Once deposited, nanoparticles (NPs) or ''ultrafine'' particles often remain in the lung lining fluid until dissolution (assuming they are soluble), escaping both phagocytic and mucociliary clearance mechanisms (5–8). Thus, deposition of drug-bearing NPs in the lungs may offer the potential for sustained drug action and release throughout the lumen of the lungs, not only in the deep lung or alveolar region, where macrophage clearance occurs. However, the utility of NPs for drug release is severely limited because of their low inertia, which causes them to be predominantly exhaled from the lungs after inspiration (10, 11). Moreover, their small size leads to particle–particle aggregation, making physical handling of NPs difficult in liquid and dry powder forms; this is a common practical problem that must be overcome before using NPs for oral drug delivery (12, 13). As a result of these limitations, NPs are not presently being explored commercially or clinically as vehicles for drug delivery in the lungs.

We have developed a form of particle for drug delivery that combines the advantages of LPPs and NPs while avoiding their limitations. We use spray drying (14) to form LPPs comprised of NPs held together by physical means, such as Van der Waals forces, or within a matrix of additional ingredients such as biopolymers or phospholipids. These large porous NP (LPNP) aggregates have the same physical and delivery properties as LPPs, yet, once deposited in the lungs (or placed in a physiological or physiological-like environment), they disassociate to yield NPs, with their inherent attractive features for drug delivery.

Materials and Methods

Materials. 1,2-Dipalmitoyl-sn-glycero-3-phosphocholine [DPPC, molecular weight (MW) = 734.05] and 1,2-dimyristoyl-sn-glycero-3-phosphoethanolamine (DMPE, MW = 635.86) were purchased from Genzyme; they had a purity ≥99%. Lactose monohydrate (4-O-β-galactopyranosyl-D-glucose, MW = 360.31), hydroxypropylcellulose (MW approx. 95,000), sodium phosphate monobasic monohydrate (MW = 137.99), and ammonium bicarbonate (MW = 79.06) were purchased from Spectrum Laboratory Products (New Brunswick, NJ); they had a purity ≥99%. Trizma base (purity ≥99.9%) and BSA fraction V (MW = 66,000, BSA approximately 99%) were purchased from Sigma-Aldrich. Distilled water USP grade was purchased from B. Braun Medical (Irvine, CA), and ethanol USP grade was purchased from PharmCo (Brookfield, CT). Aqueous suspensions of surfactant-free carboxylate-modified polystyrene (PS) NPs, with diameters of 25 ± 3, 170 ± 8, and 1,000 ± 66 nm as reported by the supplier, were purchased from Interfacial Dynamics (Portland, OR). Aqueous suspensions (pH = 9) of Nyacol 9950 colloidal silica, with a diameter of ≈100 nm, were purchased from EKA Chemicals (Marietta, GA).

Solution Preparation. Solutions of NPs were prepared by mixing ethanol and water (70:30 vol/vol) to the desired wt/vol fraction. Solutions of DPPC-DMPE-lactose (with or without NPs) were prepared by dissolving 0.6 g DPPC and 0.2 g DMPE in 700 ml ethanol, and heating the mixture to 60°C while stirring until it became clear. In addition, 0.210 g lactose monohydrate was dissolved in 300 ml water. Both solutions were then mixed together. If desired, PS NPs were added directly to the solution, and the resulting mixture was spray dried. In the case of silica NPs, water was replaced by 25 mM Tris buffer (pH = 9.25) to ensure colloidal silica stability. The buffer was prepared by dissolving 2.93 g Trizma base in a liter of water, and the pH was adjusted to 9.25 by adding 1 M HCl. The lactose-containing buffer was mixed with the lipid/ethanol solution, and then colloidal silica was added. Solutions of BSA were prepared by dissolving 3.255 g BSA and 0.245 g sodium phosphate monobasic in 800 ml water, while stirring. The pH of the solution was adjusted to 7.4 by adding 1 N KOH. Then, 15 g ammonium bicarbonate was dissolved in the mixture, and 200 ml ethanol was mixed with the resultant solution. PS NPs were then added directly to the solution. All solutions were used immediately after preparation.

This paper was submitted directly (Track II) to the PNAS office.

Abbreviations: LPP, large porous particle; NP, nanoparticle; LPNP, large porous NP; DPPC, 1,2-dipalmitoyl-sn-glycero-3-phosphocholine; MW, molecular weight; DMPE, 1,2-dimyristoyl-sn-glycero-3-phosphoethanolamine; PS, polystyrene; SEM, scanning electron microscopy.

‡To whom reprint requests should be addressed. E-mail: dedwards@deas.harvard.edu.

Spray-Drying Conditions. We spray dried solutions with a Niro Atomizer Portable spray drier (Columbia, MD). Compressed air with variable pressure (1–5 bars) ran a rotary atomizer located above the dryer with a drying air flow rate of 98 kg/h. Spray-dried particles were collected with a 6-inch cyclone. Three sets of conditions were used. During SD1 conditions, the inlet temperature was fixed at 110°C, the outlet temperature was about 46°C, a V24 wheel rotating at 20,000 rpm was used, and the feed rate of the solution was 70 ml/min. During SD2 conditions, the inlet temperature was fixed at 95°C, the outlet temperature was about 53°C, a V24 wheel rotating at 33,000 rpm was used, and the feed rate of the solution was 40 ml/min. For spray drying BSA solutions, the inlet temperature was fixed at 118°C, the outlet temperature was about 64°C, a V4 wheel rotating at 50,000 rpm was used, and the feed rate of the solution was 30 ml/min, with a drying-air flow rate of 100 kg/h.

Characterization of the Spray-Dried Powders. The geometric diameter of the spray-dried powders was measured by light diffraction (Rodos, Sympatec, Lawrenceville, NJ) at an applied pressure of 2 bars. The mass mean aerodynamic diameter was measured with an Aerosizer (TSI, St. Paul), which uses a time-of-flight measurement. The mass mean aerodynamic diameter (d_{aer}) is related to the geometric diameter d, assuming particle sphericity, by the formula (15): $d_{aer} = d\sqrt{\rho}$, where ρ is the particle density normalized by the density of water (1 g/cm^3). A two-stage Anderson Cascade Impactor (ACI-2, Thermo Andersen, Smyrna, GA) was used to determine fine particle fraction of selected powders. In practice, a capsule containing 10 ± 0.25 g of powder was placed in a hand-held, dry-powder, breath-activated inhaler device (the AIR inhaler) (16). The capsule was punctured, a pump simulated an inspiration (60l/min during 2 s), and the powder was deposited on different glass fiber filters depending on the aerodynamic diameter of the particles. The filters were weighed before and after the experiment; the fractions of particles with an aerodynamic diameter below 5.6 μm and below 3.4 μm were determined from the deposited weights. Scanning electron microscopy (SEM) was performed with a Leo 982 (Leo Electron Microscopy, Thornwood, NY) operating between 1 and 5 kV with a filament current of about 0.5 mA. Liquid samples were deposited on carbon conductive double-sided tape (Structure Probe, West Chester, PA) and dried in an oven at 70°C; powder samples were sprinkled on the tape and dusted. In both cases, samples were coated with a gold layer by using a Polaron (Watford, U.K.) SC7620 sputter coater, operated for 90 s at a sputtering current of 18 mA.

Redissolution of the Powder. The powder made only of NPs was redissolved in a mixture of ethanol/water (70:30 in volume) by vortexing the dry powder in the solvent. The resultant solution was then prepared for SEM experiments as described above.

Freeze Drying of the NPs. The PS NP solution (170 nm ± 8 nm) provided by Interfacial Dynamics was quickly frozen by using liquid nitrogen and then freeze dried by using a Modulyo freeze drier (ThermoSavant, Holbrook, NY).

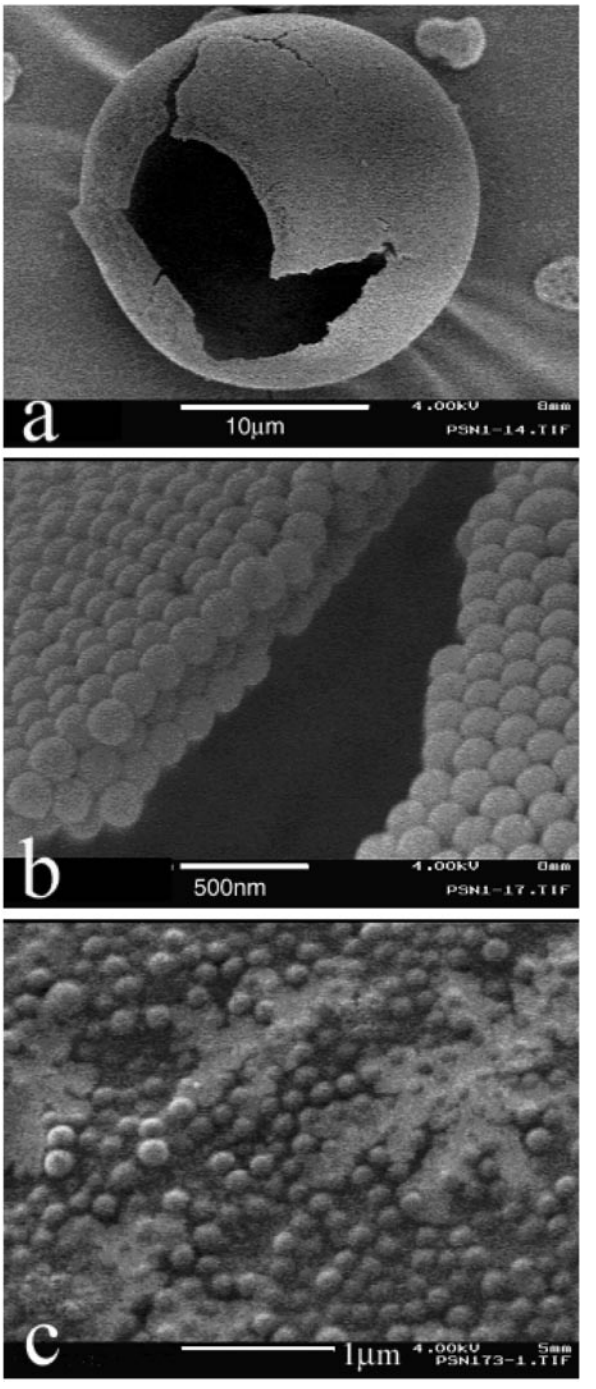

Fig. 1. SEM images of (*a*) a typical hollow sphere LPNP observed from the spray drying of a solution of PS NPs (170 nm), (*b*) a magnified view of the particle surface in *a*, and (*c*) the NPs in solution after redissolving the LPNPs in a mixture of 70:30 ethanol/water (vol/vol). LPNPs dissolve readily into the NPs once in solution.

Results and Discussion

We used SD1 spray-drying conditions to produce LPNP comprised solely of NPs (PS 170 nm, 2.3 g/liter). The LPNPs tend to be spherical and hollow as indicated by the SEM pictures in Fig. 1 *a* and *b*, with a wall thickness of approximately 400 nm, consisting of three distinct layers of NPs. These LPNPs have several attractive features: they are comprised solely of NPs; they are readily redispersed as NPs in solution (Fig. 1*c*), yet the LPNPs are readily dispersed as aerosols. To illustrate this, we aerosolized powders comprising NPs and LPNPs in separate experiments. Geometric size of the primary particles was determined by manufacturer specifications for NPs or by the limiting geometric size of the LPNPs produced at high aerosolization pressures. At all applied pressures, the NPs aggregated to a greater degree than the LPNPs, as shown in Fig. 2. Moreover the degree of aggregation depended strongly on force of aerosolization; this finding highlights some of the processing difficulties commonly associated with NP systems (12, 13).

To account for the structure of these LPNPs, we propose the following formation mechanism. Two characteristic times are crit-

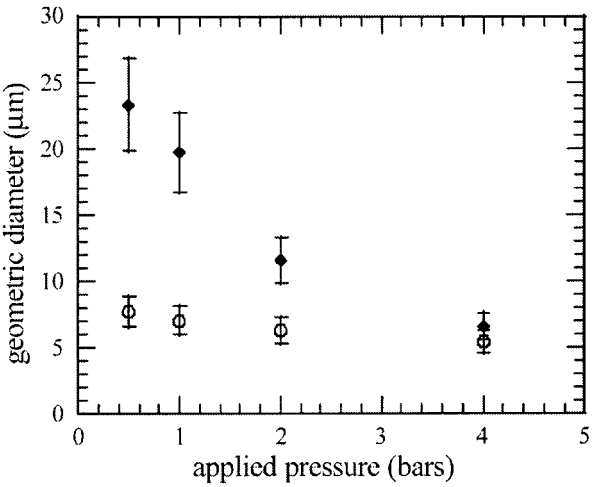

Fig. 2. Variation of the geometric size with applied pressure for freeze-dried 170-nm NPs (◆) and spray-dried LPNPs made of the same NPs (○). NPs show a strong dependence of aerosol particle size (≫170 nm) on applied pressure, illustrating their tendency to aggregate and flow with a nonlinear dependence with the stress, whereas the LPNPs show little such dependence, with a geometric size in good agreement with SEM pictures.

ical in the drying process that leads to the formation of the hollow LPNPs. The first is the time required for a droplet to dry, τ_d, while the second is the time required for a solute or a NP to diffuse from the edge of the droplet to its center, R^2/D. Here, R is the radius of the droplet and D is the solute or NP diffusion coefficient. The ratio of these two characteristic times defines an effective Peclet number, $\mathrm{Pe} = R^2/\tau_d D$, a dimensionless mass transport number that characterizes the relative importance of diffusion and convection (17). Thus, if the drying of a sprayed droplet is sufficiently slow, $\mathrm{Pe} \ll 1$, solutes or NPs within the droplet have adequate time to redistribute by diffusion throughout the evaporating droplet, yielding relatively dense dried particles. By contrast, if the drying of the droplet is very quick, $\mathrm{Pe} \gg 1$, solutes or NPs have insufficient time to diffuse from the surface to the center of the droplet, and instead accumulate near the drying front of the droplet. NPs are trapped at the free surface of the droplet in an energy well (18) resulting from the large air-water surface energy, which is greater than the difference between the particle-air and particle-water surface energies. As the droplet evaporates, and particles accumulate on the free surface, capillary forces will draw NPs together and ultimately Van der Waals forces (19–21) can lock them in place. At the end of the process the evaporating front becomes a shell or crust rich in NPs enclosing the remaining solution. This solution escapes by evaporation from the shell, pushing the NPs remaining in the drop onto the inner surface of the shell, while frequently puncturing it. This final step of the drying process is sometimes referred to as the thermal expansion phase (22).

LPNPs can also be formed with NPs of smaller sizes. This is illustrated by our creation of LPNPs using SD1 conditions with 25 nm NPs (2.3 g/liter). The SEM pictures of Fig. 3 *Upper* show a

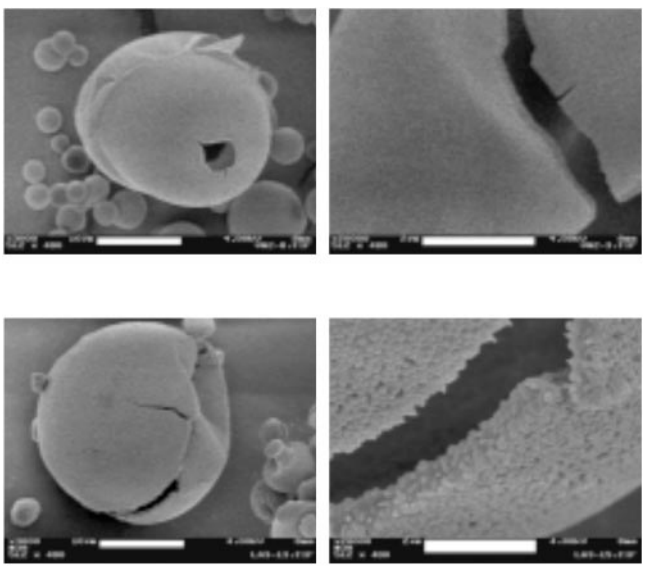

Fig. 3. SEM images of typical hollow spheres observed from the spray drying of a solution of PS NPs (25 nm, *Upper*) and a solution of lactose and PS NPs (170 nm, 70% of total solid contents in weight, *Lower*). [Scale bars: 10 μm (*Left*) and 2 μm (*Right*).]

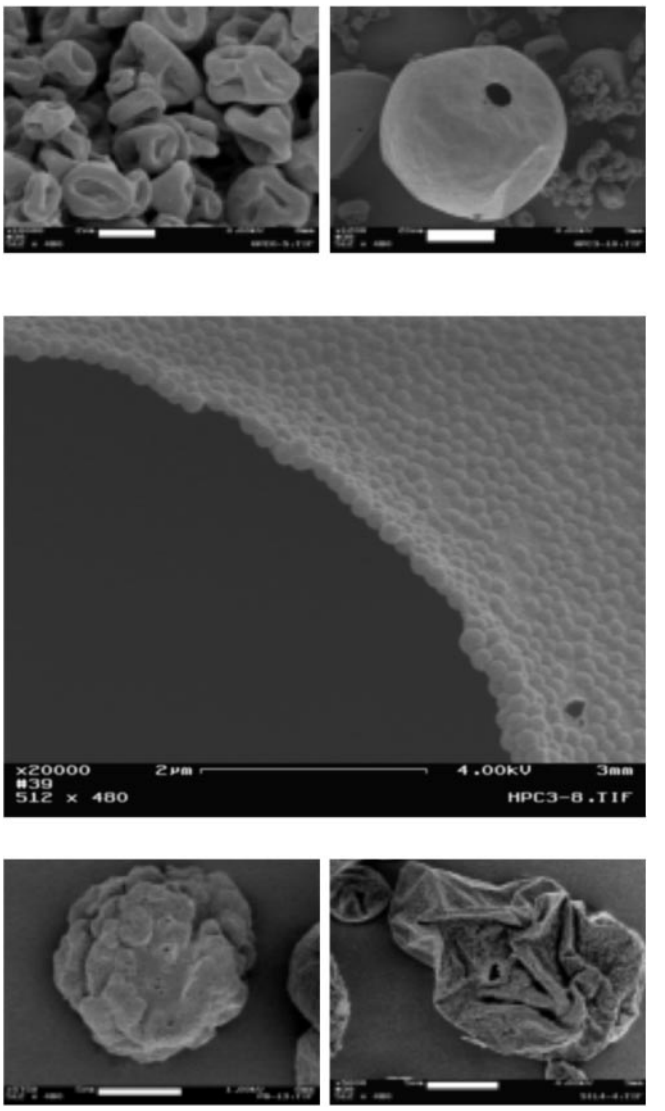

Fig. 4. SEM images of a typical hydroxypropylcellulose spray-dried particle without (*Top Left*) and with (*Top Right*) NPs. (*Middle*) A magnification of the particle surface (*Top Right*). (*Bottom*) A typical particle observed from the spray drying of a solution of BSA and PS NPs (170 nm, 80% of total solid contents in weight, *Bottom Left*), and a typical particle observed from the spray drying of a solution of lipids/lactose and colloidal silica (≈100 nm, 88% of total solid contents in weight, *Bottom Right*). [Scale bars: 2 μm (*Top Left* and *Middle*), 20 μm (*Top Right*), and 5 μm (*Bottom*).]

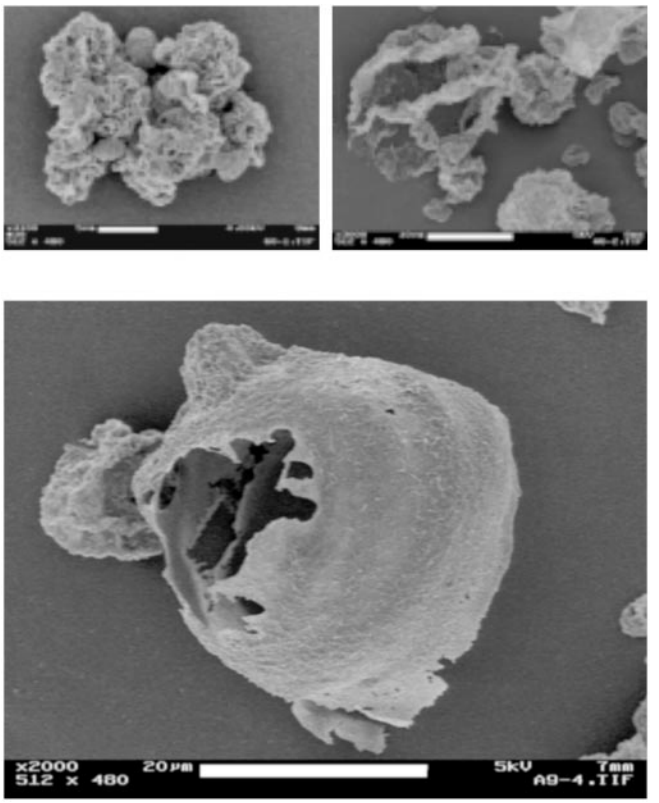

Fig. 5. SEM pictures of typical particles from the spray drying of a solution of lipids and lactose with increasing concentration of PS NPs (170 nm): 0% (*Upper Left*), 35% (*Upper Right*), and 82% of total solid content (*Lower*). [Scale bars: 5 μm (*Upper Left*), 10 μm (*Upper Right*), and 20 μm (*Lower*).]

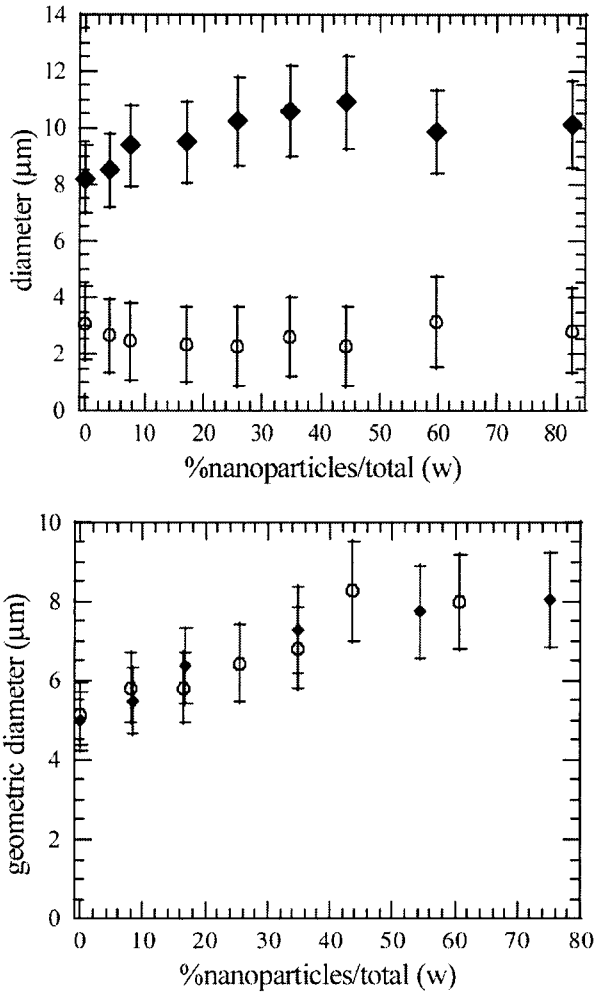

Fig. 6. (*Upper*) Variation of the mass mean aerodynamic diameter (○) and the geometric diameter (◆) of the DPPC-DMPE-lactose solution spray dried according to conditions SD1, with PS NP concentration (170 nm). (*Lower*) Variation of the geometric diameter of the DPPC-DMPE-lactose solution spray dried with SD2 conditions, with PS NP concentration (○, 25 nm; ◆, 170 nm).

LPNP particle structure similar to the one obtained with the 170-nm NPs. However, in this case, the shell thickness is approximately 200 nm and consists of eight layers of NPs. Our attempts to spray dry "NPs" as large as 1 μm in diameter did not produce the highly porous LPNPs, possibly owing to the fact that the wall formation process is hindered because the size of the suspended particles approaches that of the final spray-dried particle.

Further insight into the formation mechanism of the LPNPs and the role of the Peclet number is illustrated by the introduction of a second nonvolatile species, such as lactose, a common material in spray-dried particles (23). Using SD1 conditions, lactose [1 g/liter in 70:30 ethanol/water (vol/vol)] spray dries into relatively dense, nonporous particles whose aerodynamic diameter is 3 ± 1 μm, very close to their geometric diameter of 4 ± 0.5 μm, implying a particle mass density near unity. However, adding 70% (wt/wt) PS NPs (170 nm) to the lactose in solution, again produces high-quality LPNPs, with aerodynamic diameter 4 μm $\pm$ 2 μm and geometric diameter $d = 8 \pm 3$ μm, as illustrated in Fig. 3 *Lower*. This difference is consistent with the difference in the Peclet number. To calculate the diffusion coefficients of lactose and NPs in the fluid droplet, we use the Stokes–Einstein equation, $D_s = k_B T/(6\pi\eta R_H)$, where k_B is Boltzman's constant, η the viscosity of the solvent, T the temperature, and R_H the hydrodynamic radius of the solute ($R_H \approx 1$ nm) or NP ($R_H \approx 85$ nm). For SD1 conditions, the typical droplet radius is $R = 45$ μm, and the characteristic drying time is $\tau_d = 1$ s. This yields Pe $\approx$10 for the lactose, while Pe $\approx$2,000 for the NPs in a mixture of ethanol/water (70:30) with a viscosity of 2.3 cP. This large difference in Pe is consistent with the physical picture that the diffusive motion of the lactose is sufficiently large to prevent formation of a solid shell, whereas the much slower diffusion of the NPs allows a solid deformable shell to form, resulting in the high-quality LPNPs.

We formed LPNPs with other molecular species, too. In addition to lactose, we successfully produced LPNPs with PS NPs by using hydroxypropylcellulose, BSA, and lipids, as shown in Figs. 4 and 5. The chemical nature of the NPs also seems to be of little importance, since we successfully produced LPNPs by replacing PS NPs with colloidal silica NPs, as shown in Fig. 4 *Bottom Right*. In all cases, the LPNPs had a solid deformable shell, consisting of several layers of NPs, and had a wrinkled structure indicative of a low relative density, making their aerodynamic properties highly favorable.

To investigate the effect of the quantity of NPs on the final LPNP structure, we produced LPNPs by using a combination of three molecular constituents (DPPC, DMPE, and lactose) whose colloidal properties lead to LPP formation. Without NPs, the spray-dried particles show an excellent LPP structure, reminiscent of crumpled paper, as shown in Fig. 5. They have excellent aerodynamic properties, with $d = 8$ μm and $d_{aer} = 3$ μm. The formation mechanism of LPPs from a lipid solution is slightly different from with NPs, with the lipids spontaneously forming colloidal aggregates during the drying process. These aggregates play the role of the NPs in the shell formation process. Adding

PS NPs (170 nm) to the lipid solution produces a spray-dried particle structure that is even more crumpled. At very high NP concentrations, hollow shells are formed, as shown in Fig. 5. These qualitative observations are in accord with quantitative measurements. As shown in Fig. 6 *Upper*, we observe a 25% increase in the geometric diameter as the NP concentration increases, with the aerodynamic diameter remaining unchanged. This finding implies that the porosity of the LPNPs increases with increasing NP concentration, consistent with SEM observations. The fine particle fraction measurements performed on the same powders show that between 50% and 60% of the particles have an aerodynamic diameter below 5.6 μm and between 25% and 35% have an aerodynamic diameter below 3.4 μm, in reasonable agreement with the measured aerodynamic diameters. Thus the addition of NPs appears to improve the performance of the LPPs.

We also examined the effect of spray-drying conditions on LPNP formation. The DPPC-DMPE-lactose-NP system in ethanol/water was again spray-dried, using SD2 conditions, with varying concentrations of PS NPs (170 nm). We observed the same behavior: the aerodynamic diameter remained constant as the NP concentration increased to 75% (wt/wt), whereas the geometric diameter increased from 5 to 8 μm (Fig. 6 *Lower*). The same trend was also observed when 25-nm NPs were used, as again shown in Fig. 6 *Lower*). Thus, the formation of LPNPs appears to be generally independent of the size of the NPs, provided they are much smaller than the ultimate physical dimension of the spray-dried LPNP.

Conclusion

LPNP systems can be made of diverse materials, prepared in a variety of different conditions, and designed to deliver drugs to specific sites of the body by using NPs with diameters ranging from 25 nm to several hundred nm. They appear to be robust drug delivery systems that may be useful for encapsulating drugs of varying chemistry and molecular weight into biodegradable NPs (24), thereby combining the persistence advantages of NPs with the delivery convenience of LPPs. Their ultimate practical utility for drug delivery requires incorporation of drug, exploration of the use of other biocompatible materials, and delivery to human and animals.

We thank A. D. Dinsmore for fruitful discussions and the help of J. Sung, J. Katstra, and D. Chen during the spray-drying experiments.

1. Edwards, D. A., Hanes, J., Caponetti, G., Hrkach, J., BenJebria, A., Eskew, M. L., Mintzes, J., Deaver, D., Lotan, N. & Langer, R. (1997) *Science* **276,** 1868–1871.
2. Edwards, D. A. (2002) *AIChE J.* (2002) **48,** 2–6.
3. French, D. L., Edwards, D. A. & Niven, R. W. (1996) *J. Aerosol Sci.* **27,** 769–783.
4. Dunbar, C., Hickey, A. & Holzner, P. (1998) *KONA* **16,** 7–45.
5. Kawaguchi, H., Koiwai, N., Ohtsuka, Y., Miyamato, M. & Sasakawa, S. (1986) *Biomaterials* **7,** 61–66.
6. Krenis, L. J. & Strauss, B. (1961) *Proc. Soc. Exp. Med.* **107,** 748–750.
7. Rudt, S. & Muller, R. H. (1992) *J. Controlled Release* **22,** 263–271.
8. Vanbever, R., Ben-Jebria, A., Mintzes, J., Langer, R. & Edwards, D. A. (1999) *Drug Dev. Res.* **48,** 178–185.
9. Oberdörster, G. (2001) *Int. Arch. Occup. Environ. Health* **74,** 1–8.
10. Heyder, J., Gebhart, J., Rudolf, G., Schiller, C. & Stahlhofen, W. (1986) *J. Aerosol Sci.* **17,** 811–825.
11. Heyder, J. & Rudolf, G. (1994) *J. Aerosol Sci.* **15,** 697–707.
12. Hinds, W. C. (1998) *Aerosol Technology: Properties, Behavior, and Measurement of Airborne Particles* (Wiley, New York).
13. Kabbaj, M. & Phillips, N. C. (2001) *J. Drug Targeting* **9,** 317–328.
14. Masters, K. (1991) in *Spray Drying Handbook* (Wiley, New York).
15. Gonda, I. (1991) in *Topics in Pharmaceutical Sciences*, eds. Crommelin, D. J. A. & Midha, K. K. (Medpharm Scientific, Stuttgart), pp. 95–115.
16. Edwards, D. A. & Dunbar, C. (2002) *Annu. Rev. Biomed. Eng.* **4,** 93–107.
17. Stroock, A. D., Dertinger, S. K. W., Ajdari, A., Mezic, I., Stone, H. A. & Whitesides, G. M. (2002) *Science* **295,** 647–651.
18. Pieranski, P. (1980) *Phys. Rev. Lett.* **45,** 569–572.
19. Velev, O. D., Furusawa, K. & Nagayama, K. (1996) *Langmuir* (1996) **12,** 2374–2384.
20. Velev, O. D., Furusawa, K. & Nagayama, K. (1996) *Langmuir* **12,** 2385–2391.
21. Velev, O. D., Furusawa, K. & Nagayama, K. (1997) *Langmuir* **13,** 1856–1859.
22. Lin, J.-C. & Gentry, J. W. (2002) *Aerosol Sci. Technol.*, in press.
23. Hennigs, C., Kockel, T. K. & Langrish, T. A. G. (2001) *Drying Technol.* **19,** 471–484.
24. Lamprecht, A., Ubrich, N., Hombreiro-Pérez, M., Lehr, C.-M., Hoffman, M. & Maincent, P. (1999) *Int. J. Pharma.* **184,** 97–105.